"이 논문은 1990년도 문교부지원 한국학술 진흥재단의 지방대 육성 학술연구 조성비에 의하여 연구되었음"

[논 문] 한국재료학회지
Korean Journal of Materials Research
Vol. 1, No. 3 (1991)

$Fe_{78}B_{13}Si_9$ 비정질 합금의 결정화 거동과 취성 현상

손 인 진
전북대학교 재료공학과

Crystallization and Embrittlement of $Fe_{78}B_{13}Si_9$ Amorphous Alloy

In Jin Shon
Department of Materials Engineering, Chonbuk National University Chonju, Chonbuk 560-756, Korea

요 약 $Fe_{78}B_{13}Si_9$ 비정질 합금의 결정화 거동과 취성 현상을 시차열량기 시험, x-선회절시험 및 투과 전자현미경 관찰을 통해서 조사 연구 하였다. 결정화는 두단계의 발열반응으로 진행되었으며, 첫번째 단계에서는 비정질로부터 B.C.C. 구조인 α-(Fe, Si)의 수지상이 생성되었고, 두번째 단계에서는 남아있던 비정질로부터 B.C.T 구조인 Fe_2B가 형성되었다. 에닐링 온도에 따른 시편의 파단 변형율은 비정질 상태인 약 340℃부터 급격히 감소하였다.

Abstract Crystallization and embrittlement of $Fe_{78}B_{13}Si_9$ amorphous alloy was investigated by differential scanning calorimetry, X-ray diffraction and transmission electron microscopy. The crystallization comprizes two exothermic processes. In the first crystallization stage, α-(Fe, Si) dendrites are formed from the amorphous state, and in the second crystallization, Fe_2B compounds are formed. An abrupt decrease of the fracture strain of the ribbon started from amorphous state annealed at about 340℃

1. Introduction

Fe-B-Si amorphous alloys have been developed for a potential core material for distribution and power transformer applications at high frequencies (f>50KHz)[1]. The good properties in these alloys have been shown to the result of introduction of a small amount of crystallity by suitable annealing[1]. To further the understanding of these observed features, a detailed knowledge of the crystallization behavior and kinetics in this alloy is necessary. Many studies have been made about crystallization behavior of this alloy and it is well known that the crystallization of $Fe_{78}B_{13}Si_9$ amorphous alloy results in the formation of two principal lattice phases. However, different crystallization phase for each process has been reported[2~5], that is, (a)b.c.c. α-Fe (b)b.c.c. α-(Fe, Si) (c) b.c.t. Fe_2B (d)a nonequilibrium, transient Fe_3B phase and there are few investigations on the kinetics of nucleation and embrittlement on annealing of this alloy. Therefore, in this study, attempts have been made (A) to identify the phase and morphologies, (B) to study the nucleation kinetics of each phase, and (C) to investigate specimen embrittlement on annealing of this alloy.

2. Experimental Methods

The starting material used in this study was 25mm wide and 30um thick Metglas 2605S-2 amorphous alloy ribbons obtained from Allied Chemical Co. (U.S.A) which has composition of $Fe_{78}B_{13}Si_9$. Crystallization characteristics of 90mg samples were determined, using differential scanning calorimetry under a dry argon atmosphere with various scanning heating

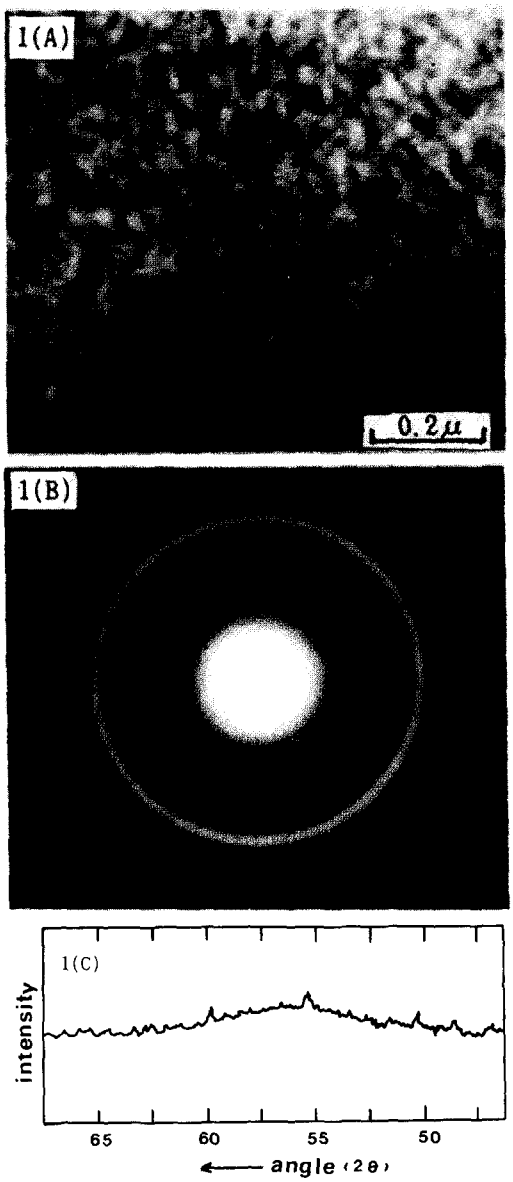

Fig. 1. Transmission electron micrograph (1A), its diffraction pattern (1B) and X-ray diffraction pattern (1C) of $Fe_{78}B_{13}Si_9$ amorphous alloy. (as-received state)

rates (2℃/min.~20℃/min.), X-ray diffraction with FeKα radiation and selected area electron diffraction in transmission electron microscopy. The activation energy of crystallization process was determined by the Kissingers peak shift method[6]. and Avrami's exponent n was calculated by the Ozawa plot[7].

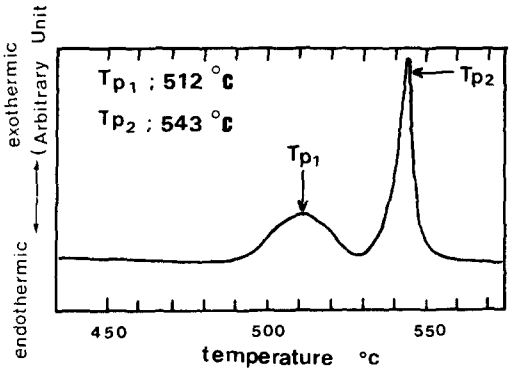

Fig. 2 DSC curve of $Fe_{78}B_{13}Si_9$ amorphous alloy (heating rate ;5℃/min.)

The fraction transformed at a temperature in the continuous heating DSC records was derived from the ratio A(T)/A(Total) under the exotherm as detailed previously[8]. Fracture strain on bending was measured by bending ribbon sample to a decreasing radius of curvature between the platens of a micrometer drive. Value of the frature strain was calculated using the platen separation at sample fracture and ribbon thickness[9].

3. Results

Microstructure of the as-cast ribbon was featureless and typical of amorphous materials (Fig. 1A). The diffraction patterns consisted of only the expected amorphous diffuse ring pattern (Fig. 1B)[10], and the amorphous state was conformed with halo pattern by X-ray diffraction (Fig. 1C). Crystallization process is shown in the DSC curve of Fig. 2. The crystallization consists of two exothermic processes, and the exothermic peaks are centered at 512 ℃ and 543℃ at the heating rate of 5℃/min. The transmission electron micrograph and diffraction pattern of the sample undergone continuous heating up to 512℃ and 543℃ with heating rate 5℃/min are shown in Fig. 3. In the first crystallization stage, α-(Fe, Si) dendrite (b.c.c) is formed from the amorphous matrix (Fig. 3A, 3B) and in the second crys-

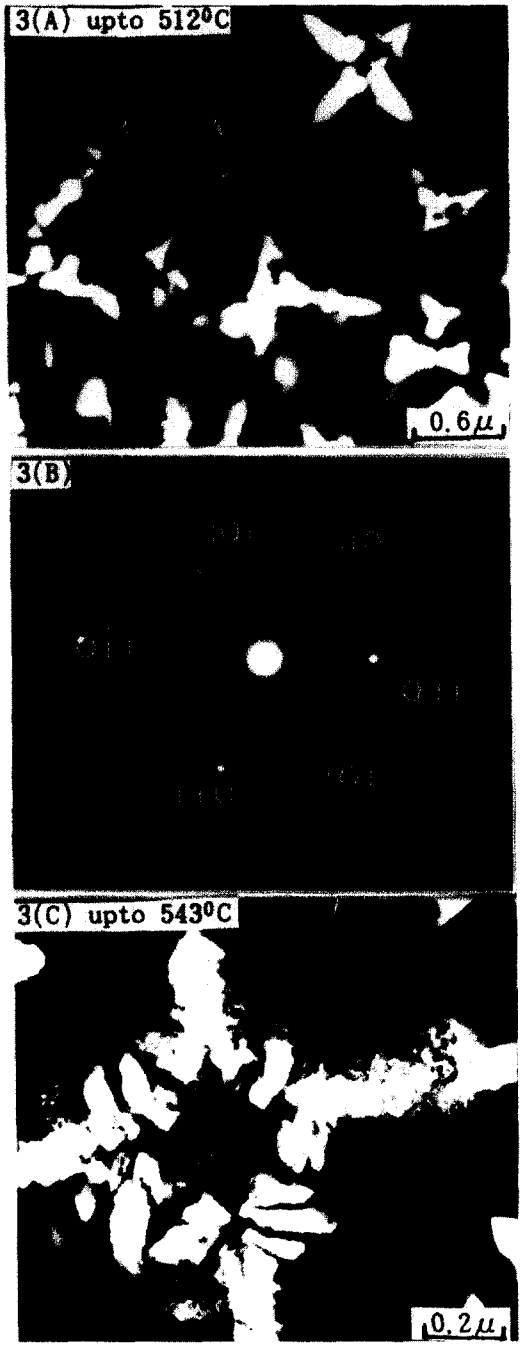

Fig. 3. Transmission electron micrograph (3A), its diffraction pattern (3B) of α-(Fe, Si) and micrograph (3C) of Fe_2B formed during continuous heating with 5°C/min.

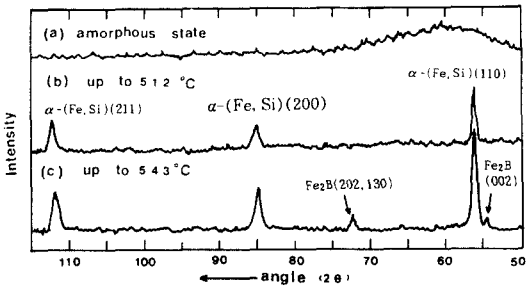

Fig. 4. The profile change in X-ray diffraction of $Fe_{78}B_{13}Si_9$ amorphous alloy after continuous heating with 5°C/min. (Fe-Kα radiation)

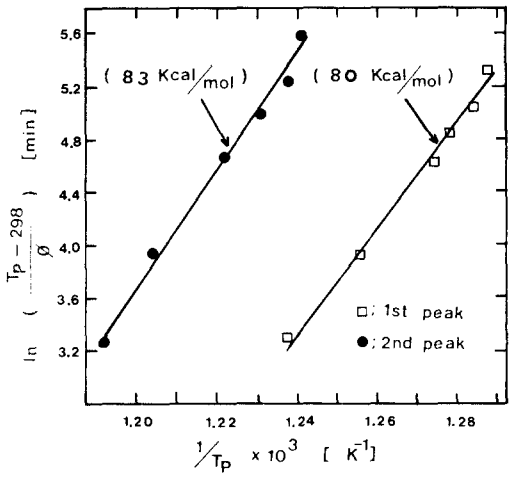

Fig. 5. Augis-Bennett plot of exothermic peak temperatures for determining activation energies of exothermic processes.(Φ: heating rate)

tallization stage, Fe_2B compound (b.c.t) of cylindrical morphology are formed from the remaining amorphous matrix (Fig. 3C). These crystal phases were also confirmed by X-ray diffraction (Fig. 4.). Augis-Bennett plot of exothermic peak temperature for determining activation energy of the exothermic process is shown in Fig. 5. The activation energies for the crystallization are about 80Kcal/mole for the formation of α-(Fe, Si) and about 83Kcal /mole for the formation of Fe_2B. Ozawa plot for determining the Avrami exponent n of first and second exothermic processes is shown in

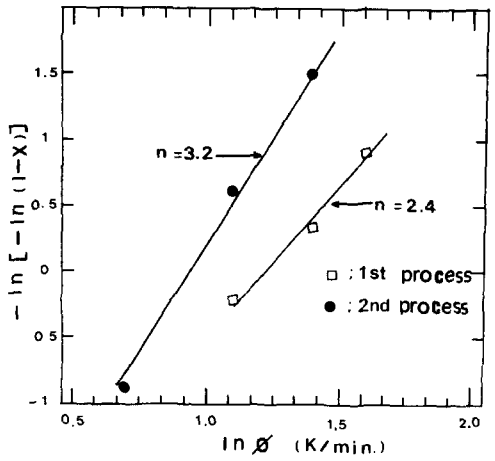

Fig. 6. Ozawa plot for determining the Avrami exponent of first and second exothermic processes. (Φ:heating rate)

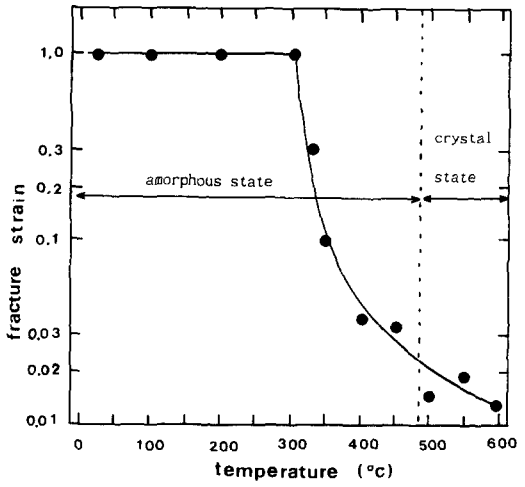

Fig. 7. Fracture strain on bending for $Fe_{78}B_{13}Si_9$ amorphous alloy ribbon heated continuously with 5℃/min.

Fig. 6. The experimental points can be fitted to a straight line and, value of exponent n and correlation coefficient b being determined by the linear regression analysis. The exponent n is about 2.4 for the α-(Fe, Si) formation and about 3.2 for the Fe_2B formation. The correlation coefficient of the linear fit is higher than 0.99 in all cases.

Fracture strain results of the specimens annealed with heating rate 5℃/min are shown in Fig. 7. An abrupt decrease of fracture strain occurs above 340℃. Such a precipitous drop in the fracture strain has been documented for some armorphous alloy systems[2, 9, 11].

4. Discussion

Diffraction angle of the primary crystallization phase in the X-ray diffraction (Fig. 4) is slightly higher than that of α-Fe, and distance of spots from origin in the electron diffraction pattern (Fig. 3) is longer than that of α-Fe. These results indicate that the lattice parameter of the primary crystallization phase becomes shorter with increasing dissolution of Si into α-Fe. Thus the primary crystallization phase can be evaluated as α-(Fe, Si) and the secondary crystallization phase Fe_2B could determined from the patterns of X-ray diffraction and electron diffraction. These results agree with those reported by Y. Ogino[3] and A. Adams[4], but are different from the results of H.H Leibermann[2] and C.F. Chang[5] who reported that first crystallized phase is α-Fe and second crystallized phase is Fe_3B instead of Fe_2B in this alloy. Crystallization consists of two steps. The first step is nucleation and the second step is grain growth. The growth of α-(Fe, Si) and Fe_2B in this alloy was reported as the diffusion controlled process[4]. And the solubility of B and Si in α-Fe at about 700°K is below 0.01 and 10 at % respectively[12]. Thus, the growth of α-(Fe, Si) and Fe_2B involves local rearrangement of Fe, Si and long range diffusion of B. The activation energy for the diffusion of the Si is 50Kcal/mole[13] and for the diffusion of the B is 37Kcal/mole[14] in this alloy. The activation energies (80Kcal/mole, 83Kcal/mole) for the crystallization are appreciably higher than activation energy for the grain growth. Therefore, the process of crystallization is mainly controlled by nucleation. The exponent n of 2.4 for the formation of α-

(Fe, Si) in the Johnson −Mehl− Avrami equation is consistent with a three demensional controlled growth and nearly constant nucleation rate regardless of time. On the other hand, for the formation of Fe_2B formation the value of n=3.2 suggests that nucleation rate of Fe_2B is increased with time. By the T.E.M observation, α−(Fe, Si) dendrite is formed in comparatively uniform way, and Fe_2B compounds are formed preferentially near the interface between α−(Fe, Si) dendrites and the remaining amorphous matrix.

The fracture strain on bending is abruptly decreased at about 340℃, and is nearly 0 above 400℃. It can be explained as follows. Amorphous state heated between 340℃ and 350℃ is brittle because the structure relaxation consisting of topological short range order [11] and chemical short range order[2, 3] cause the residual stress in the matrix. And crystallization of amorphous phase is very brittle because preferentially crystallized surface causes the residual stress between surface and interior, and Si segregation toward grain boundary [15] has an additional effect on the brittleness of the sample.

5. Conclusion

Crystallization of amorphous $Fe_{78}B_{13}Si_9$ results in the formation of two principal lattice phases, that is, a solid solution of α−(Fe, Si) and second phase Fe_2B precipitate in sequence. The activation energy and the exponent n in the Johnson−Mehl−Avrami equation of α−(Fe, Si) is about 80Kcal/mole and 2.4 respectivly. The α−(Fe, Si) has a dendrite shape and is formed uniformly. The activation energy and exponent n of Fe_2B is about 83Kcal/mole and 3.2 respectively. Fe_2B has a cylindrical shape and is formed preferentially near the interface between α−(Fe, Si) dendrite and the remaining amorphous matrix. The embrittlement of ribbon is started from amorphous state annealed at about 340℃ and ribbon becomes very brittle after crystallization.

Acknowledgements

This work was a part of fundamental study on high temperature amorphous alloy development supported by Korea Research Foundation, 1990. The author would like to thank Dong−Kyu Na and Kyung−Chon Lee for help in the microstructure observation by transmission electron microscopy.

References

1. R. Hasegawa, G.E. Fish and V.R.V. Ramannan, Proc. of 4th International Conference on Rapidly Quenched Metals, the Japan Institute of Metals, Sendai **929** (1982)
2. H.H. Liebermann, J. Marti, R.J. Martis and C.P. Wong, Metall. Trans. A **20A**, 63 (1989)
3. T. Yamasaki and Y. Ogino, J. Japan Inst. Matals **53**, 359(1989)
4. J.C. Rawers, R.A. Mccune, A. Adams, J. of Materals Science Letters **7**, 958(1988)
5. C.F. Chang and J. Marti, J. of Materials Science **18**, 2297(1983)
6. J.A. Augis and J.E. Bennett, J. Thermal Anal. **13**, 283(1978)
7. T. Ozawa, Polymer **11**, 150(1970)
8. H.J. Borchardt and F. Daniels, J. Am. Chem. Soc. **79**, 41(1957)
9. F.E. Luborsky and J.L. Walter, J. Appl. Phys. **47**, 3648(1976)
10. W. Parrish, Encyclopedia of Materials Sience and Engineering. MIT Press **5500** (1986)
11. T. Yamasaki and T. Honda and Y. Amemiya, J. Japan Inst. Metals **54**, 362 (1990)
12. M. Hansen, Constitution of Binary Alloys, 27d ed., McGraw−Hill, New York **1108** (1958)
13. F.E. Luborsky and F. Baconi, Proc. 4th

Int. Conf. on Rapidly Quenched Metals, The Japan Institute of Metals, Sendai **561** (1981)

14. V.R.V. Ramannan and G.E.Fish, J. Appl. Phys. **53**, 2273(1982)
15. H.H. Liebermann, J. Marti, R.J. Martis, and C.P.Wong, Metallurgical Transactions 20A, **63**,(1989)